Surgical and Radiologic Anatomy (2019) 41:523–528
https://doi.org/10.1007/s00276-018-2153-7

ORIGINAL ARTICLE

Anatomy of the pterygopalatine fossa: an innovative metrical assessment based on 3D segmentation on head CT-scan

Daniele Gibelli[1] · Michaela Cellina[2] · Stefano Gibelli[3] · Annalisa Cappella[1] · Marta Maria Panzeri[4] · Antonio Giancarlo Oliva[2] · Giovanni Termine[3] · Claudia Dolci[1] · Chiarella Sforza[1]

Received: 1 September 2018 / Accepted: 7 December 2018 / Published online: 12 December 2018

Abstract

Purpose The pterygopalatine fossa is an important anatomical structure for several surgical and anaesthesiologic procedures; yet, very few data are available about its size. This study aims at providing a metrical assessment of pterygopalatine fossa through an innovative 3D segmentation procedure on head CT-scans.

Methods CT-scans from 100 patients (50 males and 50 females) aged between 18 and 85 years were chosen for the study. Right and left pterygopalatine fossae were segmented through ITK-SNAP open source software. Height and volume were calculated on the acquired 3D models. In addition, anterior–posterior nasal spine distance, upper facial height (nasion–prosthion) and biorbital breadth (ectoconchion–ectoconchion) were measured as well. Statistically significant differences of height and volume according to sex and side were assessed through two-way ANOVA test: sexually dimorphic measurements were further assessed through one-way ANCOVA test using the three cranial measurements as covariates ($p < 0.05$).

Results On average pterygopalatine fossa height was 24.1 ± 3.5 mm in males, and 22.8 ± 3.4 mm in females, whereas volume was 0.930 ± 0.181 cm^3 in males and 0.817 ± 0.157 cm^3 in females, with statistically significant differences according to sex ($p < 0.05$), but not to side ($p > 0.05$); interaction was negligible for both the measurements. ANCOVA test verified that sexual dimorphism of both measurements is independent from general cranial size ($p < 0.05$).

Conclusions The present study highlighted the sexual dimorphism of pterygopalatine fossa: results may improve the knowledge of this anatomical structure difficult to explore, but crucial in several fields of clinics and surgery.

Keywords Anatomy · Pterygopalatine fossa · CT-scan · 3D segmentation

Introduction

Pterygopalatine fossa (PPF) is a pyramidal space among maxillary, sphenoid and palatine bones [1]. It communicates with the infratemporal fossa laterally through the pterygomaxillary fissure, with the orbital apex anteriorly through the medial part of the inferior orbital fissure, with the middle cranial fossa posteriorly and superiorly through the foramen rotundum, with the oral cavity inferiorly through the greater palatine foramen, and with nasal cavities medially through the sphenopalatine foramen [1]. PPF contains maxillary division branches of the trigeminal nerve, the pterygopalatine ganglion, the vidian nerve, the last segment of the maxillary artery and few emissary veins in a fatty matrix [2].

PPF is a natural crossroad among different anatomical structures linked to intracranial, facial, oral and neck spaces. Therefore, it is of clinical importance in difference fields: for example, it may be invaded by tumors or infections from all the communicating spaces because of incomplete bone boundaries [2–4]. Moreover, ligation of the sphenopalatine artery, terminal branch of the internal maxillary artery, is crucial in case of posterior epistaxis or haemostasis in surgical interventions of the cranial base [1]. PPF is also the main target of several neurosurgical procedures, including

✉ Daniele Gibelli
daniele.gibelli@unimi.it

1 Dipartimento di Scienze Biomediche per la Salute, Università degli Studi di Milano, V. Mangiagalli 31, Milan, Italy

2 Reparto di Radiologia, Ospedale Fatebenefratelli, ASST Fatebenefratelli Sacco, Milan, Italy

3 Reparto di Otorinolaringoiatria, Ospedale Fatebenefratelli, ASST Fatebenefratelli Sacco, Milan, Italy

4 Reparto di Radiologia Diagnostica, IRCCS Ospedale San Raffaele, Milan, Italy

Gamma Knife treatment of cluster headache [5], and of anaesthesiologic procedures such as maxillary nerve block [3, 6–8], where the precise knowledge of PPF anatomical characteristics is mandatory.

However, despite the importance of PPF in many surgical procedures, the exact anatomical characteristics of this structure are far from being known in depth, starting from the anatomical limits themselves [9]: for example, the superior limit is stated as the inferior orbital fissure [5, 10] or the orbital apex [11] according to different authors.

Even less data are available about the size of PPF, especially for what concerns volume: the few available studies were performed on dry skulls using impression material, placed into the cranium to occupy the entire fossa [8, 10]. However, more precise indications concerning shape and size of PPF can be obtained through 3D segmentation techniques on CT-scan, which allow operators to obtain 3D models of different anatomical structures [12, 13]. This procedure extracts a 3D reconstruction of the region of interest, and automatically calculates surfaces areas and volumes, adding more information than the traditional direct exploration of dry skulls or cadavers [12]. However, at our knowledge only one article has assessed the volume of PPF on 3D segmented models so far, on a population of 50 subjects [14].

This retrospective study aims at investigating the anatomy of the PPF through the metrical analysis of 3D segmented models extracted from 100 CT-scans, equally divided between male and female subjects: moreover, covariate analysis was applied to verify the influence of cranial size in determining possible differences between males and females. Results may help in improving data concerning this incompletely known anatomical structure.

Materials and methods

One hundred patients (50 males and 50 females) aged between 18 and 85 years (mean 42.3 ± 15.7 years in males, 49.3 ± 21.7 years in females), who had previously undergone a maxillofacial CT-scan in 2017 were chosen for the study. No significant age difference existed between sexes (Student's t test, $p > 0.05$). The most frequent clinical requests for CT-scan were screening for cranial fractures in traumatic injuries (57.3%), sinusitis or nasal and paranasal symptoms (20.0%), and neurological symptoms (12.7%). Patients affected by pathological conditions (tumors, etc.) or traumatic injuries affecting PPF were excluded from the study.

CT-scans were anonymized according to local and international ethic rules. The study follows guidelines by Helsinki Declaration.

All CT-scans were performed on a second generation dual-source scanner, Somatom Definition Flash (Siemens, Forchheim, Germany); parameters of acquisition: kV: 120, mAs: 320, collimation: 40×0.6 mm, tube rotation: 1 s; reconstruction thickness: 3 mm; reconstruction filters: H21s smooth for soft tissues and H60 sharp for bone.

The segmentation of PPF fossa from the 100 CT-scans was performed through ITK-SNAP open source software [12, 13]: in detail, the perimeter of PPF was manually selected slide by slide (Fig. 1). The anterior and posterior segmentation limits were identified in the posterior wall of the maxillary sinus, and in the pterygoid process of the sphenoid bone and foramen rotundum, respectively; anterolateral and medial boundaries were the pterygomaxillary fissure, and the perpendicular plate of the palatine bone with the sphenopalatine foramen, respectively, whereas the inferior limit was identified in the superior opening of the greater palatine canal. Pterygomaxillary fissure, greater palatine canal and vidian canal were not included, as the segmentation procedure was stopped at their respective openings into the PPF (Fig. 2).

The 3D models of the pterygopalatine fossa were then further analysed through a 3D elaboration software (VAM software, version 2.8.3, Canfield Scientific Inc., Figs. 3, 4). On the 3D models PPF height and volume were calculated. The entire procedure from 3D segmentation to measurement of height and volume was repeated by the same and another operator for ten models: intra- and inter-observer errors were assessed through relative technical error of measurement (rTEM).

In addition, on the same CT-scans three cranial measurements on three axes were extracted, including distance between anterior and posterior nasal spine, upper facial height (nasion–prosthion) and biorbital breadth (ectoconchion–ectoconchion).

Normal distribution and homoscedasticity of height and volume measurements were tested through Jarque–Bera and Bartlett's test, respectively, ($p < 0.05$) through routines written in Matlab® software.

Statistically significant differences according to side (factor 1) and sex (factor 2) for both measurements were assessed through two-way factorial ANOVA test ($p < 0.05$): sexually dimorphic measurements were further assessed through one-way ANCOVA test using each of the three cranial measurements as covariate ($p < 0.05$). In case of no significant differences according to side, ANCOVA test was applied to measurements taken on the right side.

Results

Intra- and inter-observer relative technical error of measurement (rTEM) was 4.0% and 1.9% for volume, 2.9% and 2.4% for height, respectively.

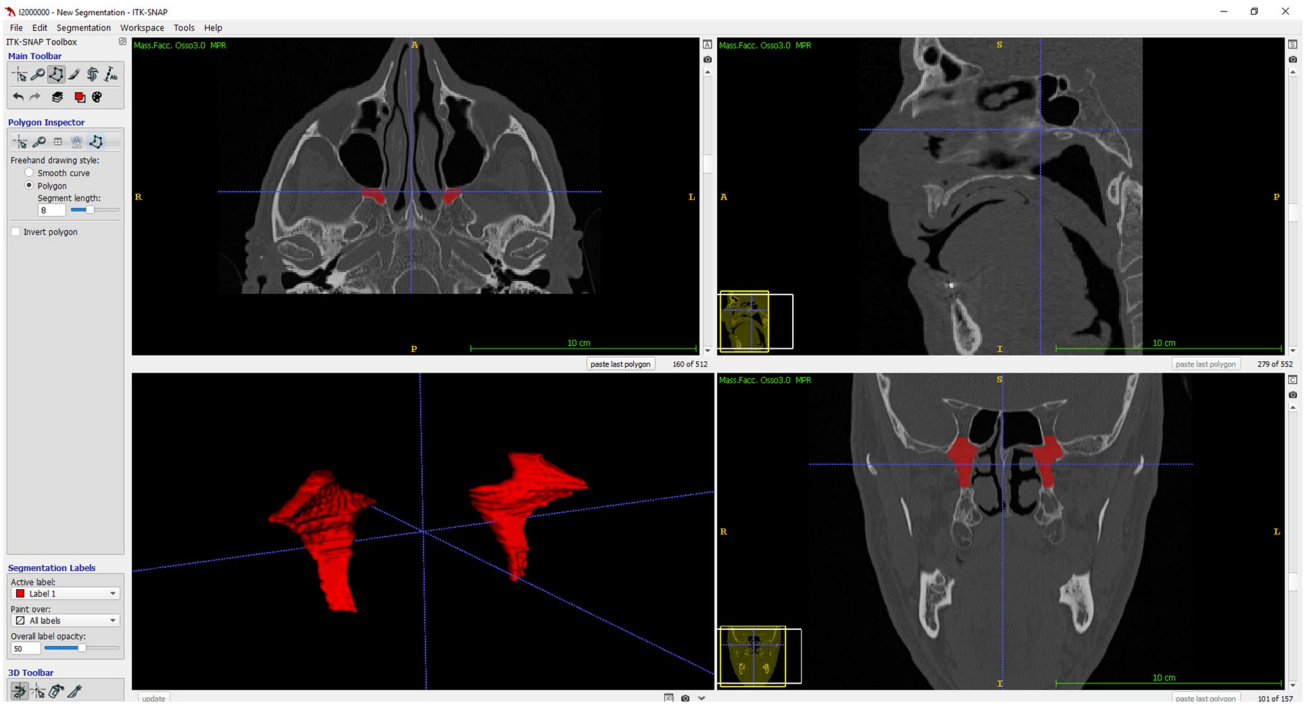

Fig. 1 Example of 3D segmentation of pterygopalatine fossae through ITK-SNAP software: PPF visualization in the three axes and reconstruction of the segmented model

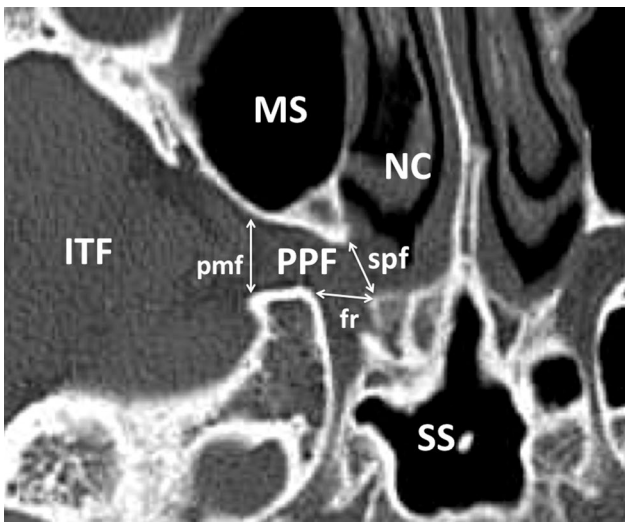

Fig. 2 Detail of PPF on CT-scan (right side). *PPF* pterygopalatine fossa, *ITF* infratemporal fossa, *NC* nasal cavity, *MS* maxillary sinus, *SS* sphenoid sinus, *pmf* pterygomaxillary fissure, *spf* sphenopalatine foramen, *fr* foramen rotundum

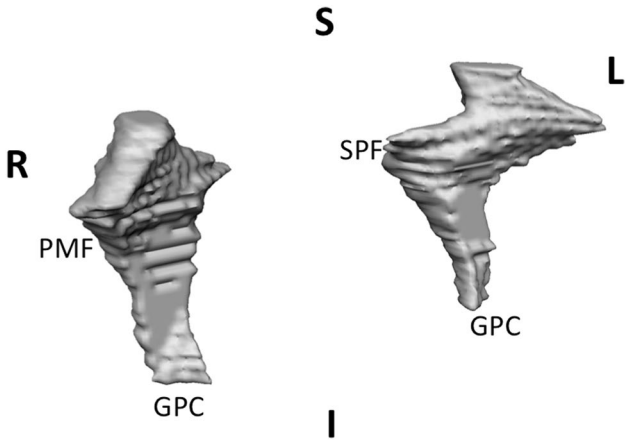

Fig. 3 Example of final 3D model of PPF. *R* right side, *L* left side, *S* superior, *I* inferior, *PMF* pterygomaxillary foramen, *SPF* sphenopalatine foramen, *GPC* superior opening of the greater palatine canal

Both height and volume showed a normal distribution and were homoscedastic ($p > 0.05$).

Overall results are shown in Table 1. Height of PPF ranged between 12.6 and 32.3 mm in males, and between 15.4 and 35.0 mm in females, being on average 1.06 times longer in males than in females. Volume ranged between 0.654 and 3.027 cm^3 in males, and between 0.510 and 2.462 cm^3 in females. The male to female volume ratio was 1.14.

Both measurements showed statistically significant differences according to sex ($p < 0.05$), but not to side; interaction between sex and side was negligible in both cases ($p > 0.05$).

Results of ANCOVA test are shown in Table 2: both height and volume were statistically significant different between males and females independently from cranial size in three axes ($p < 0.05$).

Discussion

The study of PPF is acquiring a growing importance, especially in surgical fields; in fact, tumors involving PPF are increasing by years, and surgical procedures in this area are challenging for the abundant content in vessels and nerves [15]. Research in novel surgical endoscopic accesses is increasing as well, aiming at gaining the highest surgical freedom and exposure of PPF. Three common endoscopic paths to PPF are described in literature, including the ipsilateral endonasal transmaxillary (passing through the medial and posterior portion of the maxillary sinus), the ipsilateral sublabial (through the anterior and posterior walls of the maxillary sinus, via incision of the buccogingival sulcus) and the contralateral transseptal transmaxillary approach (which needs previously the creation of a transeptal windows) [15, 16]. The application of these approaches is based on anatomical data concerning the shape and position of PPF to avoid possible injuries to vessels and nerves [15]; volume of PPF has a crucial

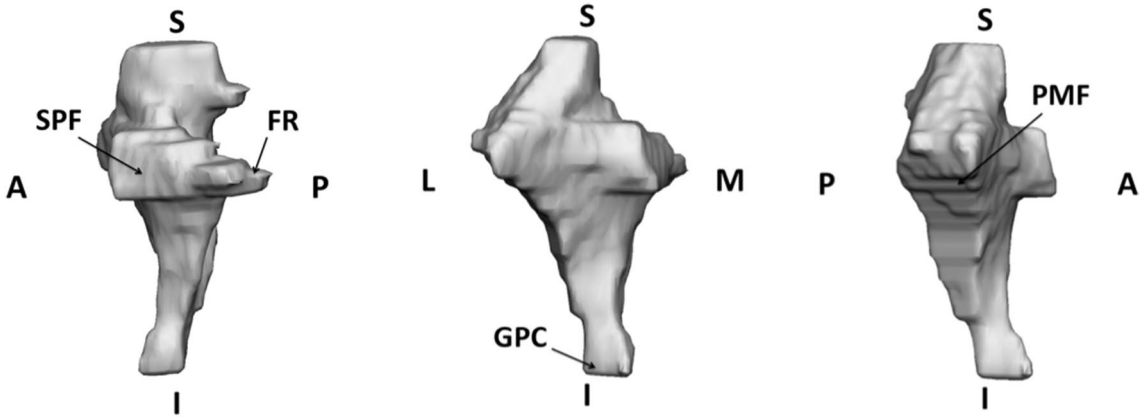

Fig. 4 Detail of PPF 3D model in different views: on the left side, medial view; in the middle, frontal view; on the right side, lateral view. *S* superior, *I* inferior, *A* anterior, *P* posterior, *L* lateral, *M* medial, *SPF* sphenopalatine foramen, *FR* foramen rotundum, *GPC* superior opening of the greater palatine foramen, *PMF* pterygomaxillary fissure

Table 1 Descriptive statistics and results of two-way ANOVA test for height and volume

	Males		Females		Total		Two-way ANOVA test					
							Sex		Side		Interaction	
	Right	Left	Right	Left	Right	Left	*F*	*p*	*F*	*p*	*F*	*p*
Height (mm)*												
Mean	24.3	23.9	22.4	23.1	23.4	23.5	7.72	0.006	0.1	0.7522	0.99	0.321
SD	3.2	3.7	3.2	3.6	3.3	3.7						
Volume (cm^3)*												
Mean	0.936	0.924	0.820	0.814	0.878	0.871	22.05	< 0.0001	0	1	0	1
SD	0.171	0.193	0.168	0.148	0.178	0.185						

*Statistically significant differences according to sex ($p < 0.05$)

Table 2 Results of one-way ANCOVA test for height and volume from the right side for all the chosen covariates ($p < 0.05$)

	Anterior–posterior nasal spine		Nasion–prosthion		Ectoconchion–ectoconchion	
	F	*p*	*F*	*p*	*F*	*p*
Height	5.511	0.021	7.845	0.006	7.449	0.008
Volume	11.269	0.001	11.576	0.001	9.833	0.002

importance as well, as it may influence the surgical freedom during endoscopic procedures.

Yet, very few data are available on PPF anatomy, as also highlighted by discussion on description and terminology of its different parts [17–19]. In addition, understanding the shape of PPF is challenging, as cadaveric dissections do not enable a full visualization of PPF, and still represents an enigmatic and "mysterious" structure not only for anatomy students, but even for aspiring surgeons and radiologists [20, 21]. The introduction of modern 3D segmentation procedures may provide a more precise visualization of PPF through three-dimensional models from CT-scan and NMR (nuclear magnetic resonance) examinations. Recently Bannon et al. applied 3D segmentation and printing technologies to PPF, obtaining a physical model in 2:1 scale, useful for didactic purposes; in this way students can appreciate directly this structure which cannot be visualized on traditional anatomical mannequins [20].

The widespread diffusion of 3D analysis methods has allowed researchers to perform more precise studies concerning not only shape, but also volume of PPF, crucial especially for anaesthesiologic procedures. In fact, usually 3 ml is the recommended dosage for maxillary block [3], and 2 ml is suggested for the control of bleeding during endoscopic sinus surgery [22]. However, these indications are based on empirical findings, and some patients may experience adverse events, including headache [7] or even brainstem anaesthesia [23]. Three-dimensional analysis of PPF provides the exact volumetric measurement, and consequent possible explanation to the adverse events previously described. In fact, in the present population the average PPF volume was lower than 1 ml and, therefore, the fossa may not be able to accommodate the dose of local anaesthetic suggested by literature, with consequent invasion of the middle cranial fossa through the foramen rotundum [8]. Therefore, 3D assessment of PPF may be useful for a correct assessment of anaesthetic dosage in surgical practice.

The first studies aiming at assessing the volume of PPF were based on the insertion of impression material (such as silicone gel) in dry skulls. Gallardo et al. first attempted at measuring the volume of 71 dry skulls and found a mean value of 1.2 ml, slightly higher than those found in the present study [24].

Stojcev Stajcic et al. repeated the same procedure on 85 dried skulls [8]; their median volume was lower than the mean PPF volume reported in our study (0.70 cm^3 versus 0.930 cm^3 in males, 0.817 cm^3 in females): in addition, height was lower as well (17–18 mm versus 23.9–24.3 mm in males, 22.4–23.1 in females). These discordances may be due to different procedures of volume extraction and may be explained by difficulties in removing the PPF cast from dry skulls; moreover, PPF limits are not defined with precision and, therefore, results are not fully comparable to the present ones. From this point of view, 3D segmentation procedure provides a faster and more reliable volumetric assessment of PPF than physical methods, as shown also by the high intra- and inter-observer repeatability. Moreover, CT scanning is not destructive, and may be performed on dry skulls as well. Furthermore, none of the previously cited articles has evaluated possible statistically significant differences according to sex. On the other side, no statistically significant differences according to side were observed [8, 24].

Hwang et al. first applied 3D segmentation techniques to reconstruction of three-dimensional models of PPF to calculate height and volume in 50 patients [14]. Although they applied the same technique and define similar limits of PPF, their volume was higher than that found in the present study (1039.9 cm^3), whereas height was lower (21.0 mm). Indeed, the present study expanded the previous investigation [14], increasing the sample and including the assessment of side, whereas the previous study applied statistical analyses to a pooled sample including both the right and left structures [14]. In addition, possible influence of cranial size was first tested through the measurement of three cranial measurements and the application of covariate test.

Sexual dimorphism of PPF is confirmed and proved that it is wider in males than in females. Moreover, statistical analyses proved that both measurements are independent from general cranial size which is a known justification for sexual dimorphism. From a practical point of view, these results have important consequences, as they justify the possible modification of anaesthesiologic procedures according to the sex of patients.

Moreover, the comparison with existing literature suggests that PPF volume vary according to different populations, as well as its shape: in fact, the Korean population studied by Hwang et al. had a shorter PPF with a higher volume than the current Italian one, suggesting the possible influence of ethnic variability [14]. From a clinical point of view this result may be helpful for the correction of anaesthetic dosage according not only to sex, but also to the ethnic origin of patients.

This study has some limitations: first of all, the lack of precise limits of PPF is an obstacle for 3D assessment of this anatomical structure. Secondarily, the possible influence of surrounding structures such as the maxillary and sphenoid sinuses [17] may have an influence in determining the volume of PPF and will be verified by further studies.

Conclusions

The present article provided data concerning volumes of PPF obtained through 3D segmentation on CT-scans. Volume ranged between 0.654 cm^3 and 3.027 cm^3 in males, and between 0.510 cm^3 and 2.462 cm^3 in females. Results give a

contribution for explaining the adverse effects of maxillary nerve block procedures in some patients and are useful for the adjustment of volume of local anaesthetic injected into the PPF according to the sex of the patient.

Acknowledgements The authors thank Ms. Annalisa Gadler for data collection.

Author contributions DG: project development, data collection, data analysis, manuscript writing, manuscript editing. MC: project development, data collection, data analysis, manuscript writing, manuscript editing. SG: project development, data collection, manuscript editing. AC: data analysis, manuscript writing, manuscript editing. MMP: data analysis, manuscript editing. AGO: data collection, manuscript editing. GT: data collection, manuscript editing. CD: data analysis, manuscript editing. CS: project development, data analysis, manuscript editing.

Compliance with ethical standards

Conflict of interest The authors declare that they have no competing interests.

References

1. Roberti F, Boari N, Mortini P, Caputy AJ (2007) The pterygopalatine fossa: an anatomic report. J Craniofac Surg 18:586–590
2. Tashi S, Purohit BS, Becker M, Mundada P (2016) The pterygopalatine fossa: imaging anatomy, communications, and pathology revisited. Insights Imaging 7:589–599
3. Allen GD (1984) Dental anaesthesia and analgesia (local and general). Williams and Wilkins, Baltimore
4. Cavallo LM, Messina A, Gardner P, Esposito F, Kassam AB, Cappabianca P, de Divitiis E, Tschabitscher M (2005) Extended endoscopic endonasal approach to the pterygopalatine fossa: anatomical study and clinical considerations. Neurosurg Focus 19:E5
5. Alvernia JE, Spomar DG, Olivero WC (2007) A computed tomography scan and anatomical cadaveric study of the pterygopalatine ganglion for use in Gamma Knife treatment of cluster headache. J Neurosurg 107:805–808
6. Sareen D, Agarwal AK, Kaul JM, Sethi A (2005) Study of sphenoid sinus anatomy in relation to endoscopic surgery. Int J Morphol 23:261–266
7. Stajcic Z, Todorovic LJ (1997) Blocks of the foramen rotundum and the oval foramen: a reappraisal of extra oral maxillary and mandibular nerve injections. Br J Oral Maxillofac Surg 35:328–333
8. Stojcev Stajcic L, Gacic B, Popovic N, Stajcic Z (2010) Anatomical study of the pterygopalatine fossa pertinent to the maxillary nerve block at the foramen rotundum. Int J Oral Maxillofac Surg 39:493–496
9. Rusu MC, Didilescu AC, Jianu AM, Paduraru D (2013) 3D CBCT anatomy of the pterygopalatine fossa. Surg Radiol Anat 35:143–159
10. Erdogan N, Unur E, Baykara M (2003) CT anatomy of pterygopalatine fossa and its communications: a pictorial review. Comput Med Imaging Graph 27:481–487
11. Williams PL, Gray H, Bannister LH (1999) Gray's anatomy: the anatomical basis of medicine and surgery. Churchill Livingstone, Edinburgh
12. Codari M, Zago M, Guidugli GA, Pucciarelli V, Tartaglia GM, Ottaviani F, Righini S, Sforza C (2016) The nasal septum deviation index (NSDI) based on CBCT data. Dentomaxillofac Radiol 45:20150327
13. Yushkevich PA, Piven J, Hazlett HC, Smith RG, Ho S, Gee JC, Gerig G (2006) User-guided 3D active contour segmentation of anatomical structures: significantly improved efficiency and reliability. Neuroimage 31:1116–1128
14. Hwang SH, Seo JH, Joo YH, Kim BG, Cho JH, Kang JM (2011) An anatomic study using three-dimensional reconstruction for pterygopalatine fossa infiltration via the greater palatine canal. Clin Anat 24:576–582
15. Liu MC, Yin XR, Zhang YS, Yang W, Zhang HW, Duan HB, Liu JM, Cheng KL, Li YQ (2017) Computed tomography research: relative anatomy of Caldwell–Luc approach in pterygopalatine fossa surgery. J Craniofac Surg 28:1537–1540
16. Elhadi AM, Almefty KK, Mendes GA, Kalani MY, Kalani MY, Nakaji P, Dru A, Preul MC, Little AS (2014) Comparison of surgical freedom and area of exposure in three endoscopic transmaxillary approaches to the anterolateral cranial base. J Neurol Surg B Skull Base 75:346–353
17. Craiu C, Rusu MC, Hostiuc S, Sandulescu M, Derjac-Arama AI (2017) Anatomic variation in the pterygopalatine angle of the maxillary sinus and the maxillary bulla. Anat Sci Int 92:98–106
18. Pinheiro-Neto CD, Fernandez-Miranda JC, Rivera-Serrano CM, Paluzzi A, Snyderman CH, Gardner PA, Sennes LU (2012) Endoscopic anatomy of the palatovaginal canal (palatosphenoidal canal): a landmark for dissection of the vidian nerve during endonasal transpterygoid approaches. Laryngoscope 122:6–12
19. Sluder G (1913) Etiology, diagnosis, prognosis and treatment of sphenopalatine ganglion neuralgia. JAMA 61:1201–1206
20. Bannon R, Parihar S, Skarparis Y, Varsou O, Cezayirli E (2018) 3D printing the pterygopalatine fossa: a negative space model of a complex structure. Surg Radiol Anat 40:185–191
21. Derinkuyu BE, Boyunaga O, Oztunali C, Alimli AG, Ucar M (2017) Pterygopalatine fossa: not a mystery! Can Assoc Radiol J 68:122–130
22. Wormald PJ, Athanasiadis T, Rees G, Robinson S (2005) An evaluation of effect of pterygopalatine fossa injection with local anesthetic and adrenalin in the control of nasal bleeding during endoscopic sinus surgery. Am J Rhinol 19:288–292
23. Nique TA, Bennett RC (1981) Inadvertent brainstem anaesthesia following extra oral trigeminal V2–V3 blocks. Oral Surg 51:468–470
24. Gallardo CAC, Galdames ICS, Lopez MGC, Matamala DAZ (2008) Relationship between pterygopalatine fossa volume and cephalic and upper facial indexes. Int J Morphol 26:393–396